



## Minireview: Advances in Germanium Isotope Analysis by Multiple Collector–Inductively Coupled Plasma–Mass Spectrometry

Yu-Miao Meng & Rui-Zhong Hu

To cite this article: Yu-Miao Meng & Rui-Zhong Hu (2018) Minireview: Advances in Germanium Isotope Analysis by Multiple Collector–Inductively Coupled Plasma–Mass Spectrometry, Analytical Letters, 51:5, 627–647, DOI: [10.1080/00032719.2017.1350965](https://doi.org/10.1080/00032719.2017.1350965)

To link to this article: <https://doi.org/10.1080/00032719.2017.1350965>



Accepted author version posted online: 18 Jul 2017.  
Published online: 15 Nov 2017.



Submit your article to this journal [↗](#)



Article views: 82



View Crossmark data [↗](#)



# Minireview: Advances in Germanium Isotope Analysis by Multiple Collector–Inductively Coupled Plasma–Mass Spectrometry

Yu-Miao Meng and Rui-Zhong Hu

State Key Laboratory of Ore Deposit Geochemistry, Institute of Geochemistry, Chinese Academy of Sciences, Guiyang, China

## ABSTRACT

The advent of multiple collector–inductively coupled plasma–mass spectrometry (MC-ICP-MS) has made the high-precision determination of Ge isotopes possible, which leads to the widespread application of Ge isotopes in earth, ocean, and cosmochemistry fields. This paper reviews the history of Ge isotope analysis, chemical dissolution and purification, and mass spectrometry measurements. Concentrated  $\text{HNO}_3$  is sufficient to dissolve nearly all types of samples and HF is also involved for Si-rich samples. Low-temperature ashing prior to dissolution is an alternative way to preconcentrate Ge in organic-rich samples. For different matrices, Ge isotopes can be determined by MC-ICP-MS coupled with a traditional nebulizer system or hydride generation system after two-step separation, one step cation/anion-exchange separation, or Mg/Fe co-precipitation protocols. Ion-exchange column methods are suitable for samples with elevated matrix and Ge content such as sulfides, iron oxides, silicate rocks, and coals, whereas Mg or Fe coprecipitation methods are particularly suitable for all kinds of water. Hydride generation systems are improved over traditional nebulizer system due to the smaller sample quantity and fewer matrix-related interferences. Sample-standard bracketing, double spike, and external Ga isotope normalization are used to mass bias correction and yield consistent results. Analytical methods involving Ge-poor samples and Ge isotope analyses based on different Ge species or specific Ge compound in natural environment will be important prospects in the further study. For further applications of Ge isotopes in mineral deposits such as sulfide and iron oxide deposits, sulfides, and iron oxides reference materials should be developed in the future.

## ARTICLE HISTORY

Received 29 May 2017  
Accepted 2 July 2017

## KEYWORDS

Chemical purification; germanium isotopes; interferences; multiple collector–inductively coupled plasma–mass spectrometry (MC-ICP-MS); sample digestion

## Introduction

Germanium is a scarce, but not an extremely rare element in the earth's crust (about 1.6 ppm Ge on average) (Bernstein 1985). Germanium has the outer-electron configuration  $3d^{10}4s^24p^2$  and generally occurs in the quadrivalent state. In minerals, Ge often appears in the form of the oxide ( $\text{GeO}_2$ ) or the sulfide ( $\text{GeS}_2$ ), and in solution as germanic acid,  $\text{Ge}(\text{OH})_4$  (Rosenberg 2009). Divalent Ge compounds such as GeO and GeS only can be

**CONTACT** Yu-Miao Meng  [mengyumiao@vip.gyig.ac.cn](mailto:mengyumiao@vip.gyig.ac.cn)  Institute of Geochemistry, Chinese Academy of Sciences, Guiyang 550081, China.

Color versions of one or more of the figures in the article can be found online at [www.tandfonline.com/lanl](http://www.tandfonline.com/lanl).

© 2017 Taylor & Francis

synthesized in the laboratory with difficulty and are generally not stable under atmospheric conditions or at temperatures much above 25°C (Bernstein 1985).

Germanium is unusual because it exhibits lithophilic, siderophilic, chalcophilic, and organophilic affinities in terms of different geochemical environments (Bernstein 1985). The lithophilic behavior is indicated by slight enrichment of Ge in the continental crust relative to the oceanic crust and the upper mantle (Taylor and McLennan 1985), and the coupled behavior between Ge and Si during partial melting and fractional crystallization. This siderophilic behavior of Ge is reflected by the fact that it can achieve concentration of up to 500 ppm in the iron phase of meteorites and telluric iron (Bernstein 1985; Wasson and Kimberlin 1966). The siderophilic behavior is also indicated by relatively high Ge contents (up to 250 ppm) in iron oxides such as magnetite and hematite (Meng et al. 2017). Goethite from oxide zone of Apex mine contains up to 5000 ppm Ge (Bernstein 1985). The chalcophilic property of Ge is evident for its economic level in zinc- and copper-rich sulfide hydrothermal systems. Low-iron sphalerite is the most important of all minerals containing relatively high amounts of Ge, up to 3000 ppm (Höll, Kling, and Schroll 2007; Belissont et al. 2014). Germanium has one of the highest affinities for organic matter of all elements commonly associated with carbonaceous sediments (Höll, Kling, and Schroll 2007). Due to its organophile behavior, Ge is commonly enriched in lignite and coal (Höll, Kling, and Schroll 2007; Qi et al. 2011).

Germanium has eight nuclides, among which, five naturally occurring isotopes of masses 70 (20.5%), 72 (27.4%), 73 (7.8%), 74 (36.5%), and 76 (7.8%) are all stable and are not produced by any radioactive decay (Green, Rosman, and De Laeter 1986; Rosman and Taylor 1998; Chang et al. 1999).  $^{68}\text{Ge}$ ,  $^{71}\text{Ge}$ , and  $^{77}\text{Ge}$  have very short half-lives of 270.9 days, 11.4 days, and 11.3 h, respectively (Audi et al. 1997), and are not detected in nature. Ge isotope ratios,  $^{74}\text{Ge}/^{70}\text{Ge}$ ,  $^{73}\text{Ge}/^{70}\text{Ge}$ , and  $^{72}\text{Ge}/^{70}\text{Ge}$ , were first determined by thermal ionization mass spectrometry (TIMS), but no significant variations in Ge isotope composition were detected due to the low uncertainty of several parts per million (Shima 1963; Green, Rosman, and De Laeter 1986). The advance of multiple collector-inductively coupled-plasma-mass spectrometry (MC-ICP-MS) has made the high-precision measurement of Ge isotope possible (Halliday et al. 1995). This technique was first used to analyze the Ge isotope composition of iron meteorites and provided the first direct evidence for mass-dependent fractionation of Ge isotopes (Hirata 1997; Xue et al. 1997; Luais et al. 2000). The further application of this technique involves earth, ocean, and cosmochemistry fields (Galy et al. 2003; Rouxel, Galy, and Elderfield 2006; Qi et al. 2011; Escoube et al. 2012a; Luais 2012; Belissont et al. 2014; Meng, Qi, and Hu 2015; Rouxel and Luais 2017). In these studies, multiple analytical methods and isotope standards regarding Ge isotopes are involved, which possess their own advantages in terms of different sample matrices. However, the systematic summary and comparison between different analytical methods are not sufficient, which has limited the further development of more simple and efficient Ge isotope analytical techniques.

In this paper, we summarize the recent advances in Ge isotope analytical methods from the literature and our laboratory. These advances include the history of Ge isotope analysis, chemical digestion and purification processes, mass spectrometry determination, and notation and standards of Ge isotopes. This review will provide new insights on method selection for various sample matrices and further improvement of Ge isotope analysis of samples with complex matrices.

## History of Ge isotope analysis

The determination of Ge isotopic composition spans a remarkably long history. A series of equipment, including electron bombardment ion source mass spectrometry (Reynolds 1953), thermal ionization mass spectrometry (TIMS) (Shima 1963), solid source mass spectrometry (Green, Rosman, and De Laeter 1986), secondary ionization mass spectrometry (SIMS) (Nishimura, Takeshi, and Okano 1988; Richter, Liang, and Davis 1999; Onishi et al. 2006) and gas isotope mass spectrometry (GIMS) (Kipphardt et al. 1999), have been used to evaluate Ge isotope composition. Due to the low analytical precision of about one standard deviation, these techniques are considered problematic and do not resolve meaningful variations of Ge isotopes in natural abundance.

Traditionally, TIMS has been the technique for achieving the highest accuracy and precision for isotope ratio measurements despite the involvement of extensive sample preparation and long measurement times necessary to achieve reliable data. However, due to the high ionization potential of Ge (7.899 eV) (Rosenberg 2009), the application of TIMS is limited. Inductively coupled plasma–mass spectrometry (ICP-MS) has further improved the Ge isotope measurement over TIMS due to the increased ionization efficiency of the plasma source. Xue et al. (1997) used quadrupole ICP-MS to determine the concentrations and isotope composition of Ge in iron meteorites and provided direct evidence for evaporative loss-induced Ge isotope variations during the formation of oxide rims of Canyon Diabolo spheroids. This technique involved the addition of Ga as an internal standard to correct for instrumental drift. However, the uncertainty (~0.3%) was still too high to resolve sub part per million isotope variations.

MC-ICP-MS was subsequently applied to determine Ge isotope ratios due to its high sample throughput, high mass resolution, and high precision (Hirata 1997; Luais et al. 2000). However, the much larger mass bias along with MC-ICP-MS was recognized and should be properly corrected for accurate isotope ratio measurements. The Ga-external correction technique, which allows detecting the isotopic fractionation of the elements during the sample formation, was applied for the Ge isotope analysis (Hirata 1997; Xue et al. 1997; Luais et al. 2000). The isotope ratio repeatability of a mono-elemental Ge solution was better than 0.06‰ per mass unit at the 95% confidence level (Rouxel and Luais 2017) confirming the superiority of MC-ICP-MS over other mass spectrometry techniques. Due to the high precision and sensitivity, MC-ICP-MS is thus widely used to probe subtle Ge isotope variations in low-level Ge natural matrices (Galy et al. 2003; Rouxel, Galy, and Elderfield 2006; Siebert, Ross, and McManus 2006; Luais 2007; Qi et al. 2011; Escoube et al. 2012a; Luais 2012; Belissont et al. 2014; Meng, Qi, and Hu 2015).

## Chemical digestion and purification

### Chemical digestion

Different acids were used in the digestion of different types of samples. The concentrated HNO<sub>3</sub> was widely used to dissolve sulfides (e.g., pyrite, sphalerite, galena, and chalcopyrite), Fe-oxyhydroxides, and iron meteorites and quantitatively recover Ge from the solution (Escoube et al. 2012a). After sample digestion, the solutions were evaporated in open Teflon beakers at temperatures ranging from 120°C (Meng, Qi, and Hu 2015), down to 80°C (Escoube, Rouxel, and Donard 2012) or 60°C (Luais 2007). HCl and HClO<sub>4</sub>

were avoided using in all steps of sample digestion and Ge elution due to the high volatility of Ge with halogens. It has been demonstrated that Ge is lost at 85% when  $\text{HClO}_4$  is used in the dissolution acid mixture and at 100% during evaporation in dilute or concentrated HCl even at a medium temperature of 80°C (Luais 2012). This is further confirmed by previous experiments (Kaya and Volkan 2011), which demonstrate the onset of volatilization of germanium tetrachloride ( $\text{GeCl}_4$ ) at 40°C with a maximum at 80°C (Luais 2012).

The dissolution of silicate rocks commonly involves HF during Ge isotope analysis because of the volatile  $\text{SiF}_4$ , but this dissolution step is complicated by the potential volatile behavior of Ge ( $\text{GeF}_4$ ) in a medium of HF. To prevent the volatile loss of Ge during dissolution, Rouxel, Galy, and Elderfield (2006) avoid the evaporation step and directly dilute the sample solution after HF dissolution using water to obtain a solution of about 1 M HF. Insoluble fluorides, containing mostly Ca, Mg, and Al and various trace elements (Yokoyama, Makishima, and Nakamura 1999), were further isolated from the solution by centrifugation. However, some studies have demonstrated that volatile loss of Ge is not serious when dissolution of silicate rocks by a mixture of HF and  $\text{HNO}_3$  at temperatures between 60 and 65°C (Luais 2012). This is also consistent with the conclusion that  $\text{GeF}_4$  can only form at a temperature as high as 300°C (Brauer 1965).

Organic-rich samples such as black shales and coal are not easy to dissolve using methods for silicate rocks and sulfides. Qi et al. (2011) adopted repeated dissolution of Ge-rich coals by concentrated  $\text{HNO}_3$  and repeated evaporation to guarantee complete dissolution. Qi et al. (2011) also attempted to ash the coal samples at 600°C to concentrate Ge (Querol, Fernández-Turiel, and López-Soler 1995) and demonstrated that there is no distinct Ge loss and Ge isotope fractionation during low-temperature ashing process because the combustion temperature is lower than the melting point of Ge (937.4°C). However, this situation may be quite different for the high temperature (1400°C) combustion process, which significantly fractionates Ge isotopes, with Ge isotope compositions of soot (volatile component) are distinctly lighter (up to 2.25‰ for  $\delta^{74}\text{Ge}$ ) than those of cinder (solid residue) (Qi et al. 2011).

## **Chemical purification**

### **Two-step separation method**

Two-step separation methods of both the anion- and cation-exchange resins are used to separate Ge from silicate matrices (Rouxel, Galy, and Elderfield 2006; Luais 2012). The silicate matrices (major elements such as alkalis and alkaline earths) and other soluble fluorides complexes can be attached on the cationic resin in the presence of dilute acid, which limits the amount of sample loaded to avoid resin saturation. Silicon behaves as Ge both on cationic and anionic resins (Korkisch 1988), meaning that liquid-liquid chromatography is not an appropriate method for eliminating Si. Even if the remaining Si after the dissolution step is very low (less than 0.6%) and has no isobaric interferences with Ge, it will lead to analytical difficulties in sample introduction and vaporization via nebulization during MC-ICP-MS measurements, e.g., irregular sample flow and unstable beams to block nebulization (Luais 2012). To minimize the  $\text{SiO}_2$  contribution, the sample solution is centrifuged using filter cones before loading onto the columns (Luais 2012).

Rouxel, Galy, and Elderfield (2006) developed a comprehensive chromatography method that is suitable for various types of geological samples. About 2 ml of AG

50 W -X8 cationic resin (hydrogen form, 200–400 mesh) can accommodate no more than 15 mg of silicate sample corresponding to 20 ng of Ge, and then the anion-exchange chromatographic column is filled with ~1.8 ml AG1-X8 (Bio-Rad, Hercules, CA, USA) resin, previously washed with HNO<sub>3</sub> and conditioned with 1 M HF. After adsorption of Ge on the column, 1 M HF and H<sub>2</sub>O was passed through the column to elute the remaining matrix such as transition elements (Co, Ni, Cu, Zn, and Ga), which are not attached in HF, whereas Fe (as Fe(II) or Fe(III) form) is attached slightly at very low HF molarity, but not at higher molarities ( $K_d$  increasing by ~1 log unit for molarity decreasing from 3 to 0) (Luais 2012). It is notable that Ti and Sb behave similar to Ge on anionic resin, which form stable fluoride complexes and are adsorbed on the resin, even at any molarity in nitric acid (Schindewolf and Irvine 1958; Faris and Buchanan 1964).

### ***One step cation-exchange method***

For Fe–Ni (iron meteorite and terrestrial iron formation) and ZnS matrices, because the most important matrices are cations, Ge is purified using the AG 50 W -X8 (hydrogen form, 200–400 mesh, 2 ml) cation-exchange resin (Luais 2007), which shows extremely low partition coefficients for Ge in the presence of very dilute HNO<sub>3</sub> (DeCarlo et al. 1981) and by contrast high partition coefficients for transition metal elements (Fe, Zn, Co, Ni, Cr) and Ga. Germanium is fully recovered in 2 ml of 0.5 M HNO<sub>3</sub>, whereas the transition metals and Ga remain attached on the resin. Elution of Ga, Co, Ni in the Ge fraction is negligible, whereas Fe and Zn abundances correspond to the upper limit for negligible drift in the Ge isotope ratios. Washing the columns with 10 ml of 6 M HCl fully eluted the Fe, Ni, Co, and Cr from the matrix (Luais et al. 2000; Luais 2007, 2012).

### ***One step anion-exchange method***

One step anion-exchange method was used for separating Ge from silicate and lignite matrices, and the volume of AG1-X8 anion-exchange resin was mostly 1.2–2 ml (wet volume). In the presence of very dilute HNO<sub>3</sub> media, Ge shows extremely high partition coefficients (DeCarlo et al. 1981), while the other matrix elements except for Sb show relatively low partition coefficients. The column was previously washed using 3 M HNO<sub>3</sub> and deionized water, and was then conditioned with 1 M HF. After adsorption of Ge on the column, about 10–13 ml of 1 M HF and 2 ml of deionized water passed through the column to elute the remaining matrices (Qi et al. 2011; Escoube et al. 2012a; Luais 2012). Because of negligible adsorption of Ge at any molarity in nitric acid, probably due to its occurrence as germanic acid in the loaded solution (Kraus and Nelson 1958), 0.1–0.5 M HNO<sub>3</sub> and 3 M HNO<sub>3</sub> have been shown to effectively elute Ge. Similarly, transition metal elements such as Fe, Zn, Co, Ni, Cr, Ga, and Ti are not adsorbed at any molarity of HNO<sub>3</sub> (Faris and Buchanan 1964).

### ***Mg and Fe coprecipitation method***

Due to the low concentrations of Ge species, such as inorganic Ge (~20 ng/L), methyl Ge, and dimethyl Ge in the river, seawater and hydrothermal fluid, the measurement of Ge isotope composition suffers great analytical challenges. Escoube, Rouxel, and Donard (2008) established the preconcentration method of Ge and some other ultra-trace elements from seawater. Inorganic Ge and other ultra-trace elements such as Fe are coprecipitated with magnesium present in seawater by addition of NH<sub>4</sub>OH (final pH ~9–10). Magnesium precipitates are filtered and dissolved in 0.25 M HNO<sub>3</sub>. The Mg coprecipitation method

was evaluated by processing 1 L of acidified surface seawater spiked with our Ge standard to a concentration of 50 ng/L. Procedural blanks are estimated at less than 0.4 ng/L.

Guillermic et al. (2017) recently developed a preconcentration method for determining Ge isotope composition of inorganic Ge in seawater. Germanium was coprecipitated with iron hydroxide with a yield better than ~70%. An anion exchange resin was used to further purify Ge from Fe and remove potential matrix elements interfering with Ge hydride generation. Germanium isotopes were determined by MC-ICP-MS coupled to a hydride generation system using a double-spike method. The analytical method requires a minimum Ge amount of about 2.6 ng, which is sufficient to measure the isotope composition of inorganic Ge in surface seawater.

In summary, different chemical purification methods have their merits and demerits. Two-step separate techniques are time-consuming and the recovery may sometimes be a little lower (~95%), but it is strict for the separation and purification of Ge from other elements. One step cationic- or anion-exchange process is highly efficient and provides satisfactory recoveries (>97%). However, single step anion resin purification method for Ge isotope analysis of natural sulfides is only suitable for the determination by MC-ICP-MS coupled with hydride generation system (Rouxel, Galy, and Elderfield 2006; Escoube et al. 2012a; Meng, Qi, and Hu 2015), because the remained elements Ti, Zn, Pb, and Sb in Ge-bearing solution can induce serious matrix effects. If the sample introduction system was changed, more rigorous purification method should be developed and matrix effects should be reevaluated. The Mg coprecipitation method may be only suitable for Ge separation from low matrix samples such as seawater, river water, and hydrothermal water.

## Mass spectrometry measurements

### *Cyclone or perfluoroalkoxy nebulizer systems*

The normal introduction system for the Ge isotope measurement is a cyclone or perfluoroalkoxy (PFA) nebulizer system. The standards or samples in 0.01 M HNO<sub>3</sub> are introduced in a free-aspiration mode into the MC-ICP-MS through a PFA nebulizer at a 50 µl/min flow rate (Luais 2007), and then vaporized into a chilled cyclonic spray chamber and a quartz torch. This introduction system has been considered to have considerably less fractionation due to no additional process involved during sample introduction. However, this introduce system requires high Ge concentration in solution and Ge isotopes may suffer a series of interferences if the matrix elements in analytical solution are not completely removed.

### *Hydride generation systems*

The hydride generation (HG) system is based on the reaction of many metalloid oxyanions with sodium borohydride and HCl or HNO<sub>3</sub> to produce volatile hydrides such as H<sub>2</sub>Te, H<sub>2</sub>Se, H<sub>3</sub>As, H<sub>3</sub>Sb, and H<sub>4</sub>Ge (Dedina and Tsalev 1995). The continuous flow HG system has been successfully applied for the high-precision determination of Ge, Se, and Sb isotopes (Rouxel, Ludden, and Fouquet 2003; Rouxel, Galy, and Elderfield 2006; Layton-Matthews et al. 2006; Zhu et al. 2008; Lobo et al. 2013; Lobo, Degryse, Shortland, and Eremin et al. 2014; Meng, Qi, and Hu 2015). The time of reagent mixing and the time when the volatile hydride is separated from the liquid and sent to the optical cell are very

important. After being mixed together, the liquid mixture flows through a tube of a specific length (read this as a controlled reaction time) forced by a peristaltic pump and is ultimately sent into a gas/liquid separator where the hydride and some gaseous hydrogen (produced by the  $\text{NaBH}_4 + \text{H}_2$  reaction) bubble out and are purged (through a high purity inert gas) into the optical cell via a gas transfer line (Dedina and Tsalev 1995). Most of the reagents introduced into the system flow are sent to a waste container, which should be handled carefully and labeled well because of the very high concentration of acid.

The concentrations of sodium borohydride, sodium hydroxide, and nitric acid (for most other elements use hydrochloric acid) reagents fed into the HG reaction vessel are also important. The HG agent was prepared freshly before each analytical session and was composed of 8 g of sodium borohydride powder and 4 g of sodium hydride pellets dissolved in 1 L deionized water (Rouxel, Galy, and Elderfield 2006; Meng, Qi, and Hu 2015). Optimization of the acid is important and different acids are chosen for different elements. For the determination of Ge isotope ratios, the acid media is 0.14 M  $\text{HNO}_3$ . The concentration of reagent acid is designed at producing a reproducible amount of hydride in the module. Thus, this acid concentration of hydrides is not necessarily identical with those of the samples and standards.

The major advantages of the HG-MC-ICP-MS technique are improved sensitivity, reducing the quantity of Ge in solution (as low as 10 ng), avoiding any matrix effects particularly from alkalis, and removing potential isobaric interferences (e.g., Zn). Rouxel, Galy, and Elderfield (2006) have demonstrated that the Ge isotope composition is not biased by the addition of 200 ppb Fe, 100 ppb Al, Na, K, and 10 ppb Se in 10 ppb Ge solution using HG sampling. Compared to the desolvation system used by Galy et al. (2003), the HG technique requires a tenth of Ge with a similar long-term reproducibility. In some cases, the HG system was connected with gas chromatography or cold trapping to preconcentrate Ge and lower detection limits for low-level determination of Ge species in seawater (Andreae and Froelich 1984; Hambrick et al. 1984). The HG system was also coupled with the regular cyclonic spray chamber using an extra inlet available on the spray chamber, which allows a direct comparison of instrumental mass bias induced by both techniques and the calculation of hydride yield (Rouxel, Galy, and Elderfield 2006; Escoube et al. 2012a; Meng, Qi, and Hu 2015).

## Interferences and methods to solve them

There are two main types of interferences occurring in the plasma: isobaric and polyatomic. Isobaric interferences refer to different elements whose isotopes share a common mass, whereas polyatomic interferences result from the combination of two or more isotopes from different elements which are from the sample matrix, sample diluent, and argon itself (Neubauer 2010). Germanium isotope measurement suffers from a series of interferences including polyatomic interferences  $^{35}\text{Cl}^{35}\text{Cl}$  on  $^{70}\text{Ge}$ ,  $^{40}\text{Ar}^{16}\text{O}_2$  and  $^{36}\text{Ar}^{36}\text{Ar}$  on  $^{72}\text{Ge}$ ,  $^{58}\text{Ni}^{16}\text{O}$  and  $^{38}\text{Ar}^{36}\text{Ar}$  on  $^{74}\text{Ge}$ ,  $^{38}\text{Ar}^{38}\text{Ar}$  and  $^{36}\text{Ar}^{40}\text{Ar}$  on  $^{76}\text{Ge}$  in plasma, isobaric  $^{70}\text{Zn}$  and  $^{69}\text{GaH}$  on  $^{70}\text{Ge}$ ,  $^{71}\text{GaH}$  on  $^{72}\text{Ge}$ , and isobaric  $^{74}\text{Se}$  on  $^{74}\text{Ge}$  (Table 1) (Rouxel, Galy, and Elderfield 2006; Luais 2012). Avoiding the use of HCl and  $\text{HClO}_4$  during the chemical purification has reduced the  $\text{Cl}^+$ -based interference. The application of the online HG system has minimized argon and oxygen-based matrices and the interferences from alkalis (Rouxel, Galy, and Elderfield 2006; Escoube et al.



**Table 1.** Isotope abundances and isobaric and polyatomic interferences of Ge isotopes.

Mass	68	69	70	71	72	73	74	75	76	77	78
Ge											
Ga			20.5%	39.9%	27.4%	7.8%	36.5%		7.8%		
Zn	18.8%	60.1%									
Se			0.6%								
As											
Ar, Cl, S-based			$^{40}\text{Ar}^{14}\text{N}^{16}\text{O}$ , $^{37}\text{Cl}^{16}\text{O}^{17}\text{O}$ , $^{36}\text{S}^{16}\text{O}^{18}\text{O}$ , $^{36}\text{S}^{17}\text{O}^{18}\text{O}$ , $^{36}\text{S}^{16}\text{O}_2$ , $^{34}\text{S}^{16}\text{O}_2$ , $^{34}\text{S}^{17}\text{O}_2$ , $^{34}\text{S}^{18}\text{O}_2$ , $^{36}\text{Ar}^{32}\text{S}$ , $^{35}\text{Cl}^{32}\text{S}$ , $^{54}\text{Fe}^{16}\text{O}$	$^{36}\text{Ar}^{14}\text{N}^{16}\text{O}$ , $^{35}\text{Cl}^{17}\text{O}^{18}\text{O}$ , $^{36}\text{S}^{16}\text{O}^{18}\text{O}$ , $^{36}\text{S}^{17}\text{O}^{18}\text{O}$ , $^{36}\text{S}^{16}\text{O}_2$ , $^{34}\text{S}^{16}\text{O}_2$ , $^{34}\text{S}^{17}\text{O}_2$ , $^{34}\text{S}^{18}\text{O}_2$ , $^{36}\text{Ar}^{32}\text{S}$ , $^{35}\text{Cl}^{32}\text{S}$ , $^{54}\text{Fe}^{16}\text{O}$	$^{36}\text{Ar}^{14}\text{N}^{16}\text{O}$ , $^{35}\text{Cl}^{17}\text{O}^{18}\text{O}$ , $^{36}\text{S}^{16}\text{O}^{18}\text{O}$ , $^{36}\text{S}^{17}\text{O}^{18}\text{O}$ , $^{36}\text{S}^{16}\text{O}_2$ , $^{34}\text{S}^{16}\text{O}_2$ , $^{34}\text{S}^{17}\text{O}_2$ , $^{34}\text{S}^{18}\text{O}_2$ , $^{36}\text{Ar}^{32}\text{S}$ , $^{35}\text{Cl}^{32}\text{S}$ , $^{54}\text{Fe}^{16}\text{O}$	$^{36}\text{Ar}^{14}\text{N}^{16}\text{O}$ , $^{35}\text{Cl}^{17}\text{O}^{18}\text{O}$ , $^{36}\text{S}^{16}\text{O}^{18}\text{O}$ , $^{36}\text{S}^{17}\text{O}^{18}\text{O}$ , $^{36}\text{S}^{16}\text{O}_2$ , $^{34}\text{S}^{16}\text{O}_2$ , $^{34}\text{S}^{17}\text{O}_2$ , $^{34}\text{S}^{18}\text{O}_2$ , $^{36}\text{Ar}^{32}\text{S}$ , $^{35}\text{Cl}^{32}\text{S}$ , $^{54}\text{Fe}^{16}\text{O}$	$^{36}\text{Ar}^{14}\text{N}^{16}\text{O}$ , $^{35}\text{Cl}^{17}\text{O}^{18}\text{O}$ , $^{36}\text{S}^{16}\text{O}^{18}\text{O}$ , $^{36}\text{S}^{17}\text{O}^{18}\text{O}$ , $^{36}\text{S}^{16}\text{O}_2$ , $^{34}\text{S}^{16}\text{O}_2$ , $^{34}\text{S}^{17}\text{O}_2$ , $^{34}\text{S}^{18}\text{O}_2$ , $^{36}\text{Ar}^{32}\text{S}$ , $^{35}\text{Cl}^{32}\text{S}$ , $^{54}\text{Fe}^{16}\text{O}$	$^{36}\text{Ar}^{14}\text{N}^{16}\text{O}$ , $^{35}\text{Cl}^{17}\text{O}^{18}\text{O}$ , $^{36}\text{S}^{16}\text{O}^{18}\text{O}$ , $^{36}\text{S}^{17}\text{O}^{18}\text{O}$ , $^{36}\text{S}^{16}\text{O}_2$ , $^{34}\text{S}^{16}\text{O}_2$ , $^{34}\text{S}^{17}\text{O}_2$ , $^{34}\text{S}^{18}\text{O}_2$ , $^{36}\text{Ar}^{32}\text{S}$ , $^{35}\text{Cl}^{32}\text{S}$ , $^{54}\text{Fe}^{16}\text{O}$	$^{36}\text{Ar}^{14}\text{N}^{16}\text{O}$ , $^{35}\text{Cl}^{17}\text{O}^{18}\text{O}$ , $^{36}\text{S}^{16}\text{O}^{18}\text{O}$ , $^{36}\text{S}^{17}\text{O}^{18}\text{O}$ , $^{36}\text{S}^{16}\text{O}_2$ , $^{34}\text{S}^{16}\text{O}_2$ , $^{34}\text{S}^{17}\text{O}_2$ , $^{34}\text{S}^{18}\text{O}_2$ , $^{36}\text{Ar}^{32}\text{S}$ , $^{35}\text{Cl}^{32}\text{S}$ , $^{54}\text{Fe}^{16}\text{O}$	$^{36}\text{Ar}^{14}\text{N}^{16}\text{O}$ , $^{35}\text{Cl}^{17}\text{O}^{18}\text{O}$ , $^{36}\text{S}^{16}\text{O}^{18}\text{O}$ , $^{36}\text{S}^{17}\text{O}^{18}\text{O}$ , $^{36}\text{S}^{16}\text{O}_2$ , $^{34}\text{S}^{16}\text{O}_2$ , $^{34}\text{S}^{17}\text{O}_2$ , $^{34}\text{S}^{18}\text{O}_2$ , $^{36}\text{Ar}^{32}\text{S}$ , $^{35}\text{Cl}^{32}\text{S}$ , $^{54}\text{Fe}^{16}\text{O}$	
Fe oxides											
Ni oxides											
Cr oxides											
Ca oxides											
Mn oxides											

Notes: Percent values represent the natural abundances of a specific mass; polyatomic interferences are listed only for masses related to Ge isotopes. This table was modified from Luais (2012).

2012a; Luais 2012). Using  $\text{HNO}_3$  as a reaction medium in HG system has suppressed the yields of Se and As hydride formation (Rouxel, Galy, and Elderfield 2006). A hexapole collision cell with  $\text{H}_2$  as a projectile was also used to break the polyatomic interfering species such as the argides (Luais 2007, 2012). It appears that all Ge isotopes, except  $^{76}\text{Ge}$ , can be measured without significant correction for interferences (Galy et al. 2003; Rouxel, Galy, and Elderfield 2006; Luais 2007). However, some matrix elements remained in Ge-bearing solution will significantly affect the Ge isotope measurement.

Luais (2012) has evaluated Zn, Fe, and Ni oxide interferences on the determination of Ge isotopes. A drift of -1 to -27‰ in  $\delta^{74}\text{Ge}$  values is observed without any correction for 25–0.75 ppm Zn, respectively. Zinc interferences on mass 70 are corrected using  $^{70}\text{Zn}/^{68}\text{Zn}$  of 0.0329 (Rosman 1972). Zinc interference correction has to be done, even if Ge is purified from the sample matrix through chemistry processing, as zinc is a ubiquitous contaminant element present in nearly all laboratory materials and chemical reagents. Even if Zn blanks are better than 3 ppb, this also leads to a shift of less than 0.03‰ on the  $\delta^{74}\text{Ge}$  value. Interferences of Fe oxides and Fe hydroxides on masses 72 and 73, and Ni oxides on masses 74 and 76 (Table 1) lead to shifts in Ge isotope ratios significantly greater than the analytical errors if uncorrected (Luais 2012). The determined Ge in a sample must, therefore, be free of Zn, Fe, and Ni.

Meng, Qi, and Hu (2015) evaluated the effect of different elements on Ge isotope measurements by HG-MC-ICP-MS using a standard solution doping method. Results show that no obvious isotope biases are found for Ge-bearing solutions containing significant amounts of Cu, Sn, and W even if Cu/Ge (g/g), Sn/Ge, and W/Ge ratios are up to 20, 60, and 150, respectively. However,  $\delta^{74/70}\text{Ge}$  values show obvious shifts if the solutions contain high Zn, Pb, and Sb even if Zn/Ge, Pb/Ge, and Sb/Ge ratios are low to 5, 10, and 50, respectively, which is possibly attributed to suppression of germane formation that fractionates Ge isotopes. This conclusion is consistent with previous results that Ge isotope ratios shift significantly when Zn/Ge ratios are larger than 3 (Zhu et al. 2014). Therefore, the Zn, Pb, and Sb contents in Ge-bearing solutions for Ge isotope analysis must be controlled to an enough low level.

## Mass bias correction

### Sample-standard bracketing

Mass spectrometers favor the transmission of heavier isotopes relative to lighter ones, i.e., mass bias effect, and this effect needs to be corrected (Albarède et al. 2004). To reach the highest precision and accuracy, the simplest technique is sample-standard bracketing (SSB), in which a Ge bracketing standard is measured before and after each sample (Galy et al. 2003; Rouxel, Galy, and Elderfield 2006). Standard and sample solutions should be also analyzed within 10% of the same concentration and carefully rinsed to avoid cross contamination. Temporal drift in mass bias is presumed to be constant over a short time. The bracketing standards can then be used to correct for additional instrumental mass bias by interpolating the instrumental mass bias between the two bracketing standards and applying this correction to the sample (Blum and Bergquist 2007).

Meng, Qi, and Hu (2015) used Ge standard solutions with concentrations of 5, 10, 20, and 50 ppb, which yields similar precisions of 0.19‰ (2 s,  $n = 62$ ), 0.18‰ ( $n = 38$ ), 0.16‰ ( $n = 47$ ), 0.18‰ ( $n = 28$ ), respectively, for  $^{74}\text{Ge}/^{70}\text{Ge}$  measurement. These analyses yield an

overall precision of 0.18‰ ( $n = 175$ ) for  $^{74}\text{Ge}/^{70}\text{Ge}$ , similar to 0.14‰ ( $n = 84$ ) of Rouxel, Galy, and Elderfield (2006) with SSB method. The advantage of this technique is that Ge isotopes can be analyzed in the presence of other elements which do not interfere spectrally or influence the mass discrimination.

### **Double spike**

Double spike (DS) correction can simultaneously determine the instrumental mass bias and natural fractionation factors, which can be visualized as a three-dimensional diagram where axes represent the three measured isotopic ratios. Line and plane intercepts, defined by isotope compositions of the double spike, standard solution and unknown sample measured by MC-ICP-MS, are used to determine fractionation factors between the measured and corrected isotopic ratios (Siebert, Nögler, and Kramers 2001; Albarède and Beard 2004).  $^{73}\text{Ge}$  and  $^{70}\text{Ge}$  were chosen as double spike isotopes, because potential isobaric and molecular interferences can be accounted for and their relative abundances are lower than the measured natural ratio (Siebert, Ross, and McManus 2006). The Ge isotopes used for spike production were fused from Ge oxide. The DS solution was mixed with the sample before chemical purification. The composition of the spike was adjusted to a spike/natural ratio of around 1 (g/g) (Siebert, Ross, and McManus 2006). Escoube et al. (2012a) demonstrate that a spike/natural ratio between 0.8 and 3.5 for 10 ng Ge yielded consistent results with an overall precision of 0.15‰ (2 s) for  $^{74}\text{Ge}/^{70}\text{Ge}$ . In fact, a ratio between 1 and 2 was routinely used for isotope determination.

### **External Ga isotope normalization**

The approach of using an element with mass and ionization potentials close to those of the analyte for mass bias correction has been successfully applied in high precision isotope measurements by MC-ICP-MS, such as Tl for Pb and Hg, Cu for Zn, and Sr for Zr (Albarède and Beard 2004). However, the absolute value of isotope ratio cannot be determined because of different mass discrimination for different elements. In the case of Ge, Ga is the suitable element as its isotope masses 69 and 71 bracket the Ge masses (70–76) (Hirata 1997). Moreover, the isotope composition of Ga was well established using a conventional TIMS technique (Hirata 1997). For this purpose, Ge in the samples has to be totally isolated from Ga. Germanium-bearing standard or sample is doped with the Ga international isotopic reference standard such as NBS SRM 994 ( $^{69}\text{Ga}/^{71}\text{Ga} = 1.50676$ ) (Machlan et al. 1986).

Luais (2012) evaluated three methods of mass bias correction, including sample standard bracketing, external Ga mass bias correction using the exponential law, and the empirical regression method. External Ga mass bias correction method assumed identical instrumental mass bias isotopic fractionation factors for Ga and Ge (defined as  $f_{\text{Ga}}$  and  $f_{\text{Ge}}$ , respectively), whereas the regression method assuming  $f_{\text{Ga}} \neq f_{\text{Ge}}$  but constant  $f_{\text{Ga}}/f_{\text{Ge}}$ , which is similar to the method for Cu and Zn isotope measurements (Maréchal, Télouk, and Albarède 1999). Three correction methods used for Ge isotope measurements of JMC (Johnson Matthey) and Aldrich Ge standards and meteorite samples gave the similar results within the reproducibility (Escoube et al. 2012a; Luais 2012), demonstrating the use of Ga as an appropriate element for mass bias correction of Ge. From what we have discussed above, the SSB +external Ga method is the most accurate for the normalization

(Luais 2012). The improvement of mass discrimination and isobaric interference correction, and the establishment of suitable chemical preparation methods for various types of samples make high-precision determination of Ge isotopes reliable, with an analytical reproducibility of about  $\pm 0.2\%$  and a minimum Ge quantity of  $\sim 15$  ng (Luais et al. 2000; Galy et al. 2003; Rouxel, Galy, and Elderfield 2006; Siebert, Ross, and McManus 2006; Luais 2007; 2012; Rouxel, Escoube, and Donard 2008; Yang and Meija 2010; Qi et al. 2011; Yang et al. 2011; Escoube et al. 2012a; Belissont et al. 2014; Meng, Qi, and Hu 2015).

## Notation and standards of Ge isotopes

The partitioning of stable isotopes of a certain element between two substances, A and B, is described by the isotopic fractionation factor  $\alpha$ :  $\alpha_{A/B} = R_A/R_B$ , where  $R_A$  and  $R_B$  are the ratios of the heavy to light isotopes in the molecules or phases A and B, respectively. Because  $\alpha$  is very close to 1, the very useful relationship:  $10^3 \ln \alpha_{A/B} = \delta A - \delta B = \Delta_{A-B}$  is derived, where  $\Delta_{A-B}$  is the fractionation between phases A and B, reflecting equilibrium or kinetic partitioning (Weiss et al. 2008). Equilibrium fractionation arises during isotope exchange when the forward and backward reaction rates of the isotopes that lead to isotope redistribution are identical. Kinetic fractionation occurs when the reaction is unidirectional and reaction rates are mass-dependent. Fractionation exists because bonds with the lighter isotope and lower atomic mass are broken faster. A very important kinetic fractionation process, Rayleigh distillation fractionation (RDF), occurs when reaction products are irreversibly separated from the reactant reservoir, potentially leading to extreme fractionation (Weiss et al. 2008). No mass-independent fractionation (MIF) of Ge isotopes has been found up to now.

The basics of stable isotope fractionation are well established and reviewed elsewhere (Criss 1999). In the following section, the most important principles for Ge isotopes are summarized. Because isotope variations in nature are relatively small, differences are expressed as ‰ deviations relative to a reference standard in  $\delta$  unit, where  $\delta > 0$  is considered heavy and  $\delta < 0$  light, if the heavier isotope is in the numerator.

$$\delta^{x/y}\text{Ge}(\text{‰}) = \left( \frac{({}^x\text{Ge}/{}^y\text{Ge})_{\text{sample}}}{({}^x\text{Ge}/{}^y\text{Ge})_{\text{standard}}} - 1 \right) \times 1000 \quad (1)$$

where  $X$  equals 74, 73, or 72 and  $y$  equals 70 or 72.  $\delta^{74/70}\text{Ge}$  (also  $\delta^{74}\text{Ge}$ ) is now commonly used to express Ge isotope composition due to the larger natural abundances and less isobaric interferences of masses 74 and 70. Currently, there is no consensus in Ge isotope standard used to express Ge isotope composition of natural samples. Individual laboratories have used in-house standards to calculate ‰ deviations, i.e., JMC (Lot#301230S, Johnson Matthey, Karlsruhe), Aldrich (Lot#01704 KZ, Milwaukee, WI, USA), Aristar (VWR International, West Chester, PA, USA), Spex (Lot#11-160GE, CLGE9-1AY, [Ge] = 10  $\mu\text{g}/\text{ml}$   $(\text{NH}_4)_2\text{GeF}_6$  in  $\text{H}_2\text{O}/\text{tr HF}$ ), Merck (1.70320.0100, [Ge] = 1000  $\text{mg}/\text{L}$ ) and NIST SRM3120a (Lot#000411, 1000  $\mu\text{g}/\text{g}$ ). Escoube, Rouxel, and Donard (2012) and Luais (2007) recommended NIST SRM3120a as international Ge isotope analysis standard, due to its low matrix effects and similar Ge isotope composition to the bulk silicate Earth (BSE) (Qi et al. 2011; Escoube et al. 2012a; Luais 2012; Meng, Qi, and Hu 2015).

To improve interlaboratory comparisons, Rouxel and Luais (2017) recently proposed that Ge isotope ratios of samples should be reported as  $\delta^{74/70}\text{Ge}$  values relative to NIST

**Table 2.** Average compositions of Ge isotope standards from Aristar, JMC, Spex, Aldrich, and Merck, normalized against NIST SRM3120a isotopic standard.

Lab	Introduction system	Correction method	Numbers of analyses	$\delta^{74/70}\text{Ge}$ (‰)	2 s
Aristar standard				<b>-0.64</b>	<b>0.18</b>
Woods Hole Oceanographic Institution, USA	Hydride generation	Sample-sample bracketing	11	-0.58	0.12
Woods Hole Oceanographic Institution, USA	Hydride generation	External Ga normalization	11	-0.57	0.08
The French Research Institute for Exploitation of the Sea, France	Cyclonic spray chamber	Sample-sample bracketing	4	-0.59	0.02
The French Research Institute for Exploitation of the Sea, France	Cyclonic spray chamber	Double spike	4	-0.61	0.11
Centre for Petrographic and Geochemical Research, France	Cyclonic spray chamber	External Ga normalization	6	-0.76	0.28
Centre for Petrographic and Geochemical Research, France	Cyclonic spray chamber	Sample-sample bracketing	6	-0.75	0.28
JMC standard				<b>-0.32</b>	<b>0.10</b>
Woods Hole Oceanographic Institution, USA	Hydride generation	Sample-sample bracketing	4	-0.33	0.33
Woods Hole Oceanographic Institution, USA	Hydride generation	External Ga normalization	4	-0.31	0.29
The French Research Institute for Exploitation of the Sea, France	Cyclonic spray chamber	Sample-sample bracketing	4	-0.23	0.02
The French Research Institute for Exploitation of the Sea, France	Cyclonic spray chamber	Double spike	4	-0.32	0.07
Centre for Petrographic and Geochemical Research, France	Cyclonic spray chamber	External Ga normalization	8	-0.37	0.04
Centre for Petrographic and Geochemical Research, France	Cyclonic spray chamber	Sample-sample bracketing	8	-0.37	0.16
Spex standard				<b>-0.71</b>	<b>0.20</b>
Woods Hole Oceanographic Institution, USA	Hydride generation	Sample-sample bracketing	1	-0.59	ND
Woods Hole Oceanographic Institution, USA	Hydride generation	External Ga normalization	1	-0.60	ND
Woods Hole Oceanographic Institution, USA	Hydride generation	Sample-sample bracketing	5	-0.84	0.16
Woods Hole Oceanographic Institution, USA	Hydride generation	External Ga normalization	5	-0.81	0.11
State Key Laboratory of Ore Deposit Geochemistry, China	Hydride generation	Sample-sample bracketing	27	-0.70	0.19
The French Research Institute for Exploitation of the Sea, France	Cyclonic spray chamber	Sample-sample bracketing	3	-0.61	0.04
The French Research Institute for Exploitation of the Sea, France	Cyclonic spray chamber	Double spike	4	-0.63	0.13
Centre for Petrographic and Geochemical Research, France	Cyclonic spray chamber	External Ga normalization	10	-0.81	0.19
Centre for Petrographic and Geochemical Research, France	Cyclonic spray chamber	Sample-sample bracketing	10	-0.79	0.18
Laboratory of Bioinorganic Analytical and Environmental Chemistry, France	Cyclonic spray chamber	Sample-sample bracketing	14	-0.64	0.42
Laboratory of Bioinorganic Analytical and Environmental Chemistry, France	Cyclonic spray chamber	External Ga normalization	14	-0.79	0.18
Aldrich standard				<b>-2.01</b>	<b>0.23</b>
The French Research Institute for Exploitation of the Sea, France	Cyclonic spray chamber	Sample-sample bracketing	4	-1.88	0.03
The French Research Institute for Exploitation of the Sea, France	Cyclonic spray chamber	Double spike	4	-2.14	0.06
The French Research Institute for Exploitation of the Sea, France	Hydride generation	Double spike	6	-1.90	0.10
Centre for Petrographic and Geochemical Research	Cyclonic spray chamber	External Ga normalization	84	-2.08	0.26
Centre for Petrographic and Geochemical Research, France	Cyclonic spray chamber	Sample-sample bracketing	84	-2.05	0.22
Merck standard					
State Key Laboratory of Ore Deposit Geochemistry, China	Hydride generation	Sample-sample bracketing	26	-0.36	0.08

Notes: This table was modified from Rouxel and Luais (2017). Numbers in bold represent the average of the same standard.

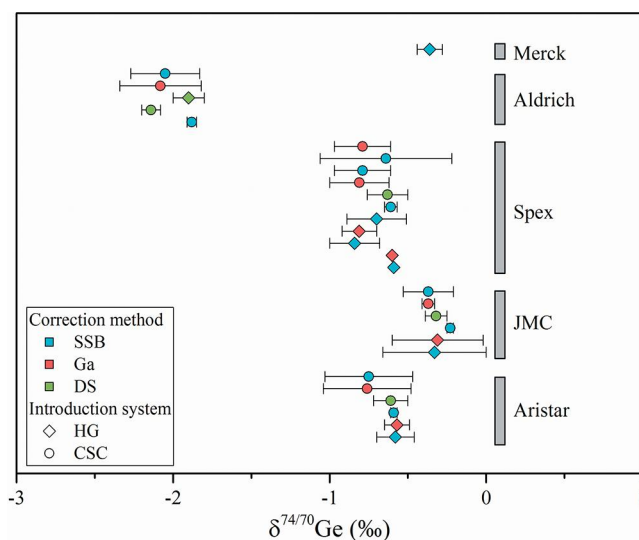


**Figure 1.**  $\delta^{74/70}\text{Ge}$  values of Ge isotope standards. Data used in this figure are compiled in Table 2. JMC, Johnson Matthey; SSB, sample-sample bracketing; DS, double spike correction; Ga, external Ga normalization; CSC, cyclonic spray chamber; HG, hydride generation.

SRM3120a which is a Ge concentration standard available with large amounts. Compiled results of Ge isotope compositions of Aristar, Spex, JMC, and Merck standards relative to SRM3120a are shown in Table 2 and are illustrated in Figure 1. Aristar and Spex solutions showed enrichment in the light isotope with the similar  $\delta^{74/70}\text{Ge}$  of  $-0.64 \pm 0.09\text{‰}$  and  $-0.71 \pm 0.10\text{‰}$ , respectively. The JMC and Merck standards also have light Ge isotope values, with similar  $\delta^{74/70}\text{Ge}$  values of  $-0.32 \pm 0.05\text{‰}$  and  $-0.36 \pm 0.08\text{‰}$ . The Aldrich standard has the lightest  $\delta^{74/70}\text{Ge}$  values of  $-2.01 \pm 0.11\text{‰}$ . There are no systematic differences in Ge isotope values using cyclonic spray chamber (CSC) or hydride generation (HG) as sample introduction systems. Different mass bias correction methods, standard-sample bracketing, external Ga normalization, and double-spike corrections, also show the similar accuracy and precision.

## Reference materials for Ge isotope

Many georeference materials were used in previous studies (Siebert, Ross, and McManus 2006; Qi et al. 2011; Escoube et al. 2012a; Luais 2012; Meng, Qi, and Hu 2015), including different types of silicate rocks (basalt, granite, dunite, peridotite, serpentine, anorthosite), glauconite, iron formation, coal, black shales, Mn nodule, and sphalerite (Table 3 and Figure 2). Basalts (BHVO-1, BHVO-2, BIR-1, BCR-1, BE-N), have relatively homogenous Ge isotope composition with an average  $\delta^{74/70}\text{Ge}$  value of  $0.55 \pm 0.16\text{‰}$  (2 s). Granitic and dioritic rocks (G-2, GH, DNC-1) are more heterogeneous relative to basaltic rocks and have  $\delta^{74/70}\text{Ge}$  values ranging from  $0.39\text{‰}$  to  $0.76\text{‰}$ . Ultramafic rocks (DTS-1, PCC-1, UB-N, AN-G) also show homogenous Ge isotope composition with an average  $\delta^{74/70}\text{Ge}$  value of  $0.64 \pm 0.18\text{‰}$  (2 s). Glauconite (GL-O) shows the heaviest Ge isotope composition with an average  $\delta^{74/70}\text{Ge}$  of  $2.44 \pm 0.13\text{‰}$  (2 s). Iron formation, coal and black shales (IF-G, CLB-1, SDO-1) have  $\delta^{74/70}\text{Ge}$  values around  $1\text{‰}$ . Pacific manganese nodule (Nod-P1) has a

**Table 3.** Compilation of Ge concentrations and isotope compositions of georeference materials reported relative to NIST SRM3120a isotopic standards.

Sample number	Sample type	Sample location	Ge (ppm)	Reference	$\delta^{47/70}\text{Ge}$ (‰)	2 s	Reference
BHVO-1	Hawaiian basalt	Hawaii, USA	1.59		0.46	0.25	
			1.64	Govindaraju (1994)	0.55	0.15	Rouxel, Galy, and Elderfield (2006)
BHVO-2	Hawaiian basalt	Hawaii, USA	1.55	Haltz (1990)	0.37	0.10	Luais (2012)
			1.58	Luais (2012)	0.53	0.12	
			1.60		0.55	0.13	Escoube et al. (2012a)
			1.52	Escoube et al. (2012a)	0.54	0.13	Escoube et al. (2012a)
			1.63	Rouxel and Luais (2017)	0.52	0.13	Escoube et al. (2012a)
			1.61	Rouxel and Luais (2017)	0.43	0.19	Escoube et al. (2012a)
			1.64	Rouxel and Luais (2017)	0.53	0.15	Escoube et al. (2012a)
					0.55	0.43	Rouxel and Luais (2017)
BIR-1	Icelandic basalt	Iceland	1.49		0.64	0.13	Rouxel and Luais (2017)
			1.5		0.51	0.2	Rouxel and Luais (2017)
			1.45		0.61	0.14	Rouxel and Luais (2017)
			1.53	Govindaraju (1994)	0.74	0.13	Escoube et al. (2012a)
				Mortlock and Frohlich (1996); Mortlock and Frohlich (1987)	0.6	0.13	Escoube et al. (2012a)
				Mortlock and Frohlich (1996); Mortlock and Frohlich (1987)	0.56	0.3	Escoube et al. (2012a)
			1.49	Haltz (1990)	0.64	0.33	Rouxel, Galy, and Elderfield (2006)
BCR-1	Columbia River basalt	Columbia River group, USA	1.52	Kurtz, Derry, and Chadwick (2002)	0.57	0.39	Rouxel, Galy, and Elderfield (2006)
			1.52		0.57	0.04	Elderfield (2006)
			1.4	Luais (2012)	0.57	0.13	Luais (2012)
			1.44	Escoube et al. (2012a)	0.55		
			1.5	Govindaraju (1994)	0.65	0.13	Escoube et al. (2012a)
BE-N	Vosges basalt	Essey-la-Côte, Nancy, France	1.42	Mortlock and Froelich (1996); Mortlock and Frohlich (1987)	0.54	0.19	Escoube et al. (2012a)
			1.45	Haltz (1990)	0.47	0.39	Escoube et al. (2012a)
			1.36	Escoube et al. (2012a)	0.54	0.22	Rouxel, Galy, and Elderfield (2006)
			1.45	Luais (2012)	0.57	0.12	Luais (2012)
G-2	Granite	Rhode Island, USA	1.16		0.55	0.14	Luais (2012)
			0.96		0.39	0.34	
			1.02				

GH	Granite	Hoggar, Algeria	0.94 0.92 1.88 2.18 1.63	Mortlock and Froelich (1996); Mortlock and Frohlich (1987) Mortlock and Froelich (1996); Mortlock and Frohlich (1987) Escoube et al. (2012a)	0.64 0.74 0.55	0.19 0.13 0.28	Rouxel, Galy, and Elderfield (2006)
DNC-1	Dolerite	Braggtown, North Carolina, USA	1.84 1.28	Luais (2012)	0.63 0.69	0.06 0.20	Escoube et al. (2012a) Rouxel, Galy, and Elderfield (2006) Luais (2012)
DTS-1	Dunite	Hamilton, Washington, USA	1.30 1.26 1.28	Govindaraju (1994) Mortlock and Froelich (1996); Mortlock and Frohlich (1987) Escoube et al. (2012a)	0.56 0.76 0.74	0.13 0.13 0.31	Escoube et al. (2012a) Escoube et al. (2012a) Rouxel, Galy, and Elderfield (2006) Rouxel, Galy, and Elderfield (2006)
PCC-1	Peridotite	California, USA	0.83 0.88 0.84	Govindaraju (1994) Halicz (1990)	0.76 0.65	0.13 0.28	Escoube et al. (2012a) Rouxel, Galy, and Elderfield (2006) Luais (2012)
UB-N	Serpentine	Col des Bagenelles, Vosges, France	0.83 0.75 0.86 0.94 0.82	Luais (2012) Escoube et al. (2012a)	0.5 0.62 0.69 0.64	0.06 0.21 0.13 0.13	Escoube et al. (2012a) Escoube et al. (2012a) Escoube et al. (2012a) Rouxel, Galy, and Elderfield (2006) Luais (2012)
AN-G	Anorthosite	Fiskenaasset, Western Greenland, Denmark	0.81 0.93	Luais (2012)	0.46 0.65	0.2 0.11	Rouxel, Galy, and Elderfield (2006) Luais (2012)
			0.93 0.86	Luais (2012) Rouxel and Luais (2017)	0.61 0.69 0.67	0.16 0.24 0.01	Luais (2012) Rouxel and Luais (2017)
			0.8 0.93	Govindaraju (1994) Halicz (1990)	0.67 0.66	0.13 0.13	Escoube et al. (2012a) Rouxel, Galy, and Elderfield (2006)

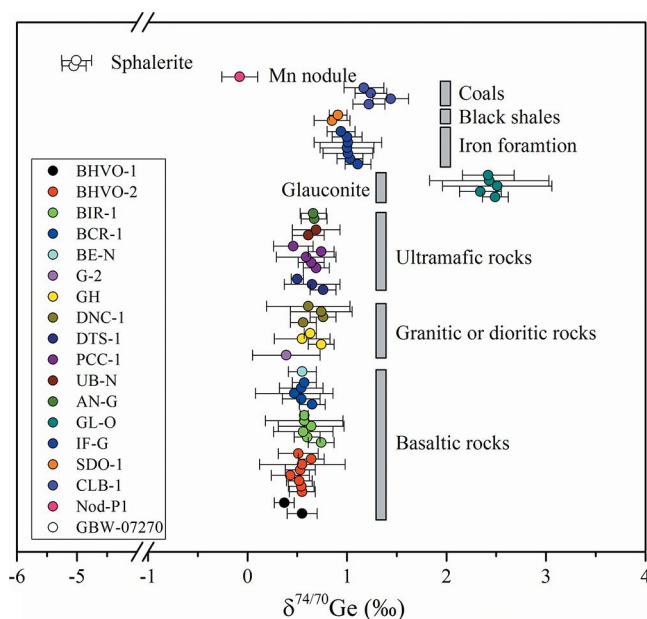
(Continued)



Table 3. Continued.

Sample number	Sample type	Sample location	Ge (ppm)	Reference	$\delta^{74/70}\text{Ge}$ (‰)	2 s	Reference
GL-O	Glauconite	Normandy, France	0.84	Escoube et al. (2012a)	2.44	<b>0.13</b>	Escoube et al. (2012a)
			4.26	Govindaraju (1994)	2.49	0.13	Escoube et al. (2012a)
			4.5	Escoube et al. (2012a)	2.34	0.21	Rouxel, Galy, and Elderfield (2006)
			4.02		2.51	0.55	Rouxel, Galy, and Elderfield (2006)
IF-G	Iron formation	Western Greenland, Denmark	23.07		2.43	0.6	Rouxel, Galy, and Elderfield (2006)
					2.42	0.26	Rouxel, Galy, and Elderfield (2006)
					1.01	<b>0.10</b>	Elderfield (2006)
SDO-1	Devonian shale	Ohio Shale near Morehead, Kentucky, USA	24	Govindaraju (1994)	1.11	0.13	Escoube et al. (2012a)
			22	Frei and Polat (2007)	1.03	0.13	Escoube et al. (2012a)
			21.8	Luais (2012)	1.01	0.25	Rouxel and Luais (2017)
			23.06	Escoube et al. (2012a)	1	0.27	Rouxel and Luais (2017)
			24.49	Rouxel and Luais (2017)	1	0.34	Luais (2012)
CLB-1	Coal	Lower Bakerstown coal bed, Castleman coal field, Maryland, USA	1.60		0.94	0.15	Rouxel and Luais (2017)
			1.56		0.88	0.14	Rouxel and Luais (2017)
			1.64		0.85	<b>0.08</b>	Rouxel and Luais (2017)
Nod-P1	Pacific Mn nodule	Deep Pacific Ocean	0.54		0.85	0.18	Rouxel and Luais (2017)
			6.67	Axelsson et al. (2002)	0.91	0.09	Rouxel and Luais (2017)
GBW-07270	Sphalerite	Taolin Pb-Zn deposit, Hunan, China			1.27	<b>0.04</b>	
					1.22	0.16	Qi et al. 2011
					1.44	0.18	Qi et al. (2011)
			1.24	0.16	0.16	Qi et al. (2011)	
			1.17	0.2	0.2	Qi et al. (2011)	
				-0.08	0.18	Rouxel and Luais (2017)	
				-5.03	<b>0.06</b>		
			7	Meng, Qi, and Hu (2015)	-5.05	0.20	Meng, Qi, and Hu (2015)
			7	Meng, Qi, and Hu (2015)	-5.01	0.25	Meng, Qi, and Hu (2015)
			6	Research Group of Sulfide Mineral Reference Materials (1995)			

Notes: This table was modified from Rouxel and Luais (2017). Numbers in bold means the average.



**Figure 2.**  $\delta^{74/70}\text{Ge}$  values of Ge isotope reference materials. These data are compiled in Table 3.

$\delta^{74/70}\text{Ge}$  value close to zero. Sphalerite reference material (GBW-07270) shows enrichment in light Ge isotopes with an average  $\delta^{74/70}\text{Ge}$  value of  $-5.03 \pm 0.06\text{‰}$  (2 s). As described above, most of the reference materials are rocks, but sulfides and oxides reference materials are lacking. For further application of Ge isotopes in mineral deposits such as sulfide and iron oxide deposits, corresponding reference materials with the same or similar matrices are needed. Therefore, it is necessary to develop sulfides (sphalerite, galena, pyrite, chalcopyrite) and oxides (magnetite, hematite) reference materials in the future.

## Conclusion and future trends

For most types of samples, there are available analytical methods for Ge isotopes including chemical dissolution and purification, and mass spectrometry measurements. However, for samples with low Ge concentration and complex matrices, modification based on the available methods is needed. The Ge species-based or compound-specific Ge isotope composition analysis would be an important aspect in the study of natural environments. The establishment of Ge isotope reference materials such as sulfides and oxides is imperative and will be beneficial to the application of Ge isotopes in the study of mineral deposits.

## Funding

This research was funded by CAS “Light of West China” Program to YMM and National Natural Science Foundation of China (41230316, 41503045). Xiaowen Huang and Jianfeng Gao from the Institute of Geochemistry, Chinese Academy of Sciences are thanked for helpful discussion during draft preparation. We also thank the reviewers for their constructive comments which have improved the manuscript.

## References

- Albarède, F., and B. Beard. 2004. Analytical methods for non-traditional isotopes. *Rev. Mineral. Geochem* 55:113–52. doi:10.2138/gsrmg.55.1.113
- Albarède, F., P. Telouk, J. Blichert-Toft, M. Boyet, A. Agranier, and B. Nelson. 2004. Precise and accurate isotopic measurements using multiple-collector ICPMS. *Geochim. Cosmochim. Acta* 68:2725–44. doi:10.1016/j.gca.2003.11.024
- Andreae, M. O., and P. N. Froelich. 1984. Arsenic, antimony, and germanium biogeochemistry in the Baltic Sea. *Tellus B* 36:101–17. doi:10.1111/j.1600-0889.1984.tb00232.x
- Audi, G., O. Bersillon, J. Blachot, and A. H. Wapstra. 1997. The NUBASE evaluation of nuclear and decay properties. *Nucl. Phys. A* 624:1–124. doi:10.1016/S0375-9474(97)00482-X
- Axelsson, M. D., I. Rodushkin, J. Ingri, and B. Öhlander. 2002. Multielemental analysis of Mn–Fe nodules by ICP-MS: Optimisation of analytical method. *Analyst* 127:76–82. doi:10.1039/B105706P
- Belissant, R., M.-C. Boiron, B. Luais, and M. Cathelineau. 2014. LA-ICP-MS analyses of minor and trace elements and bulk Ge isotopes in zoned Ge-rich sphalerites from the Noailhac–Saint-Salvy deposit (France): Insights into incorporation mechanisms and ore deposition processes. *Geochim. Cosmochim. Acta* 126:518–40. doi:10.1016/j.gca.2013.10.052
- Bernstein, L. R. 1985. Germanium geochemistry and mineralogy. *Geochim. Cosmochim. Acta* 49:2409–22. doi:10.1016/0016-7037(85)90241-8
- Blum, J. D., and B. A. Bergquist. 2007. Reporting of variations in the natural isotopic composition of mercury. *Anal. Bioanal. Chem.* 388:353–59. doi:10.1007/s00216-007-1236-9
- Brauer, G. 1965. *Handbook of preparative inorganic chemistry*. New York & London: Academic Press.
- Chang, T. L., W. J. Li, G. S. Qiao, Q. Y. Qian, and Z. Y. Chu. 1999. Absolute isotopic composition and atomic weight of germanium. *Int. J. Mass spectrum.* 189:205–11. doi:10.1016/S1387-3806(99)00081-0
- Criss, R. E. 1999. *Principles of stable isotope distribution*. New York: Oxford University Press.
- DeCarlo, E. H., H. Zeitlin, and Q. Fernando. 1981. Simultaneous separation of trace levels of germanium, antimony, arsenic, and selenium from an acid matrix by adsorbing colloid flotation. *Anal. Chem.* 53:1104–07.
- Dedina, J., and D. L. Tsalev. 1995. *Hydride generation atomic absorption spectrometry (POD)*. Chichester, UK: Wiley.
- Escoube, R., O. Rouxel, and O. F. X. Donard. 2008. Measurement of Germanium isotope composition in marine samples by hydride generation coupled to MC-ICP-MS. *EGU General Assembly: Geophys. Res. Abs.* 10:12035.
- Escoube, R., O. J. Rouxel, and O. F. X. Donard. 2012. Coupled Ge/Si and Ge isotope ratios as new geochemical tracers of seafloor hydrothermal systems: A case study at Loihi Seamount. *Geochim. Cosmochim. Acta Suppl.* 76:1305. doi:10.1016/j.gca.2015.06.025
- Escoube, R., O. J. Rouxel, B. Luais, E. Ponzevera, and O. F. Donard. 2012a. An intercomparison study of the germanium isotope composition of geological reference materials. *Geostand. Geoanal. Res.* 36:149–59. doi:10.1111/j.1751-908X.2011.00135.x
- Faris, J. P., and R. F. Buchanan. 1964. Anion exchange characteristics of the elements in nitric acid medium. *Anal. Chem.* 36:1157–58.
- Frei, R., and A. Polat. 2007. Source heterogeneity for the major components of ~3.7Ga banded iron formations (Isua Greenstone Belt, Western Greenland): Tracing the nature of interacting water masses in BIF formation. *Earth Planet. Sci. Lett.* 253:266–81. doi:10.1016/j.epsl.2006.10.033
- Galy, A., C. Pomiès, J. A. Day, O. S. Pokrovsky, and J. Schott. 2003. High precision measurement of germanium isotope ratio variations by multiple collector-inductively coupled plasma mass spectrometry. *J. Anal. At. Spectrom.* 18:115–19. doi:10.1039/b210233a
- Govindaraju, K. 1994. Compilation of working values and sample description for 383 geostandards. *Geostand. Newslett.* 18:1–158. doi:10.1046/j.1365-2494.1998.53202081.x-ii
- Green, M. D., K. J. R. Rosman, and J. R. De Laeter. 1986. The isotopic composition of germanium in terrestrial samples. *Int. J. Mass Spectrom. Ion Processes* 68:15–24. doi:10.1016/0168-1176(86)87064-1

- Guillermic, M., S. V. Lalonde, K. R. Hendry, and O. J. Rouxel. 2017. The isotope composition of inorganic Germanium in seawater and deep sea sponges. *Geochim. Cosmochim. Acta* 212:99–118. doi:10.1016/j.gca.2017.06.011
- Höll, R., M. Kling, and E. Schroll. 2007. Metallogenesis of germanium—A review. *Ore Geol. Rev.* 30:145–80. doi:10.1016/j.oregeorev.2005.07.034
- Halicz, L. 1990. Germanium contents of selected international geostandards by hydride generation and ICP-AES. *Geostand. Newslett.* 14:459–60. doi:10.1111/j.1751-908X.1990.tb00079.x
- Halliday, A. N., D. C. Lee, J. N. Christensen, A. J. Walder, P. A. Freedman, C. E. Jones, C. M. Hall, W. Yi, and D. Teagle. 1995. Recent developments in inductively coupled plasma magnetic sector multiple collector mass spectrometry. *Int. J. Mass Spectrom. Ion Processes* 146:21–33. doi:10.1016/0168-1176(95)04200-5
- Hambrick III, G. A., P. N. Froelich Jr, M. O. Andreae, and B. L. Lewis. 1984. Determination of methylgermanium species in natural waters by graphite furnace atomic absorption spectrometry with hydride generation. *Anal. Chem.* 56:421–24.
- Hirata, T. 1997. Isotopic variations of germanium in iron and stony iron meteorites. *Geochim. Cosmochim. Acta* 61:4439–48. doi:10.1016/S0016-7037(97)00273-1
- Kaya, M., and M. Volkan. 2011. Germanium determination by flame atomic absorption spectrometry: An increased vapor pressure-chloride generation system. *Talanta* 84:122–26. doi:10.1016/j.talanta.2010.12.029
- Kipphardt, H., S. Valkiers, F. Henriksen, P. De Bievre, P. D. P. Taylor, and G. Tolg. 1999. Measurement of the isotopic composition of germanium using GeF<sub>4</sub> produced by direct fluorination and wet chemical procedures. *Int. J. Mass spectrom.* 189:27–37. doi:10.1016/S1387-3806(99)00047-0
- Korkisch, J. 1988. *CRC handbook of ion exchange resins*. Boca Raton, Florida: CRC Press.
- Kraus, K., and F. Nelson. 1958. *Metal separations by anion exchange. Symposium on ion exchange and chromatography in analytical chemistry*. Atlantic City: ASTM International.
- Kurtz, A. C., L. A. Derry, and O. A. Chadwick. 2002. Germanium-silicon fractionation in the weathering environment. *Geochim. Cosmochim. Acta* 66:1525–37. doi:10.1016/S0016-7037(01)00869-9
- Layton-Matthews, D., M. I. Leybourne, J. M. Peter, and S. D. Scott. 2006. Determination of selenium isotopic ratios by continuous-hydride-generation dynamic-reaction-cell inductively coupled plasma-mass spectrometry. *J. Anal. At. Spectrom.* 21:41–49. doi:10.1039/B501704A
- Lobo, L., P. Degryse, A. Shortland, K. Eremin, and F. Vanhaecke. 2014. Copper and antimony isotopic analysis via multi-collector ICP-mass spectrometry for provenancing ancient glass. *J. Anal. At. Spectrom.* 29:58–64. doi:10.1039/C3JA50303H
- Lobo, L., P. Degryse, A. Shortland, and F. Vanhaecke. 2013. Isotopic analysis of antimony using multi-collector ICP-mass spectrometry for provenance determination of Roman glass. *J. Anal. At. Spectrom.* 28:1213–19. doi:10.1039/C3JA50018G
- Luais, B. 2007. Isotopic fractionation of germanium in iron meteorites: Significance for nebular condensation, core formation and impact processes. *Earth Planet. Sci. Lett.* 262:21–36. doi:10.1016/j.epsl.2007.06.031
- Luais, B. 2012. Germanium chemistry and MC-ICPMS isotopic measurements of Fe-Ni, Zn alloys and silicate matrices: Insights into deep Earth process. *Chem. Geol.* 334:295–311. doi:10.1016/j.chemgeo.2012.10.017
- Luais, B., X. Framboisier, J. Carignan, and J. N. Ludden. 2000. Analytical development of Ge isotopic analyses using multi-collection plasma source mass spectrometry: Isoprobe MC-HEX-ICP-MS (micromass). *Geoanalysis 2000 Symp. B* 45–46.
- Machlan, L., J. W. Gramlich, L. J. Powell, and G. M. Lambert. 1986. Absolute isotopic abundance ratio and atomic weight of a reference sample of gallium. *J. Res. Natl. Inst. Stand. Technol.* 91:323–31. doi:10.6028/jres.094.034
- Maréchal, C. N., P. Télouk, and F. Albarède. 1999. Precise analysis of copper and zinc isotopic compositions by plasma-source mass spectrometry. *Chem. Geol.* 156:251–73. doi:10.1016/S0009-2541(98)00191-0
- Meng, Y.-M., H.-W. Qi, and R.-Z. Hu. 2015. Determination of germanium isotopic compositions of sulfides by hydride generation MC-ICP-MS and its application to the Pb-Zn deposits in SW China. *Ore Geol. Rev.* 65:1095–109. doi:10.1016/j.oregeorev.2014.04.008

- Meng, Y. M., R. Z. Hu, X. W. Huang, and J. F. Gao. 2017. Germanium in magnetite: A preliminary review. *Acta Geol. Sinica* 91:711–26. doi:10.1111/1755-6724.13127
- Mortlock, R. A., and P. N. Froelich. 1996. Determination of germanium by isotope dilution-hydride generation inductively coupled plasma mass spectrometry. *Anal. Chim. Acta* 332:277–84. doi:10.1016/0003-2670(96)00230-9
- Mortlock, R. A., and P. N. Froelich. 1987. Continental weathering of germanium: Ge/Si in the global river discharge. *Geochim. Cosmochim. Acta* 51:2075–82. doi:10.1016/0016-7037(87)90257-2
- Neubauer, K. 2010. Reducing the effects of interferences in quadrupole ICP-MS. Spectroscopy. Available from: <http://www.spectroscopyonline.com/reducing-effects-interferences-quadrupole-icp-ms>
- Nishimura, H., H. Takeshi, and J. Okano. 1988. Isotopic abundances of germanium determined by secondary ion mass spectrometry. *Mass Spectrom.* 36:197–202. doi:10.5702/massspec.36.197
- Onishi, F., Y. Inatomi, T. Tanaka, N. Shinozaki, M. Watanabe, A. Fujimoto, and K. Itoh. 2006. Time-of-flight secondary mass spectrometry analysis of isotope composition for measurement of self-diffusion coefficient. *Jpn. J. Appl. Phys.* 45:5274–76. doi:10.1143/JJAP.45.5274
- Qi, H.-W., O. Rouxel, R.-Z. Hu, X.-W. Bi, and H.-J. Wen. 2011. Germanium isotopic systematics in Ge-rich coal from the Lincang Ge deposit, Yunnan, Southwestern China. *Chem. Geol.* 286:252–65. doi:10.1016/j.chemgeo.2011.05.011
- Querol, X., J. Fernández-Turiel, and A. López-Soler. 1995. Trace elements in coal and their behaviour during combustion in a large power station. *Fuel* 74:331–43. doi:10.1016/0016-2361(95)93464-O
- Reynolds, J. H. 1953. The isotopic constitution of silicon, germanium, and hafnium. *Phys. Rev.* 90:1047. doi:10.1103/PhysRev.90.1047
- Research Group of Sulfide Mineral Reference Materials. 1995. The preparation of sulphide mineral reference materials. *Rock Miner. Anal.* 14:81–113. (in Chinese)
- Richter, F. M., Y. Liang, and A. M. Davis. 1999. Isotope fractionation by diffusion in molten oxides. *Geochim. Cosmochim. Acta* 63:2853–61. doi:10.1016/S0016-7037(99)00164-7
- Rosenberg, E. 2009. Germanium: environmental occurrence, importance and speciation. *Rev. Environ. Sci. Biotechnol.* 8:29–57. doi:10.1007/s11157-008-9143-x
- Rosman, K. J. R. 1972. A survey of the isotopic and elemental abundance of zinc. *Geochim. Cosmochim. Acta* 36:801–19. doi:10.1016/0016-7037(72)90089-0
- Rosman, K. J. R., and P. D. P. Taylor. 1998. Isotopic compositions of the elements 1997. *Pure Appl. Chem.* 70:1275–88. doi:doi.org/10.1351/pac199870010217
- Rouxel, O. J., R. Escoube, and O. F. X. Donard. 2008. Measurement of Germanium isotope composition in marine samples by hydride generation coupled to MC-ICP-MS. *Geochim. Cosmochim. Acta Suppl.* 72:809. doi:1607-7962/gra/EGU2008-A-12035
- Rouxel, O., A. Galy, and H. Elderfield. 2006. Germanium isotopic variations in igneous rocks and marine sediments. *Geochim. Cosmochim. Acta* 70:3387–400. doi:10.1016/j.gca.2006.04.025
- Rouxel, O. J., and B. Luais. 2017. Germanium isotope geochemistry. *Rev. Mineral. Geochem.* 82:601–56. doi:10.2138/rmg.2017.82.14
- Rouxel, O., J. Ludden, and Y. Fouquet. 2003. Antimony isotope variations in natural systems and implications for their use as geochemical tracers. *Chem. Geol.* 200:25–40. doi:10.1016/S0009-2541(03)00121-9
- Schindewolf, U., and J. Irvine. 1958. Preparation of carrier-free vanadium, scandium, and arsenic activities from cyclotron targets by ion exchange. *Anal. Chem.* 30:906–08.
- Shima, M. 1963. Isotopic composition of germanium in meteorites. *J. Geophys. Res.* 68:4289–92. doi:10.1029/JZ068i014p04289
- Siebert, C., T. F. Nägler, and J. D. Kramers. 2001. Determination of molybdenum isotope fractionation by double-spike multicollector inductively coupled plasma mass spectrometry. *Geochem. Geophys. Geosyst.* 2. Paper number 2000GC000124. doi:10.1029/2000gc000124
- Siebert, C., A. Ross, and J. McManus. 2006. Germanium isotope measurements of high-temperature geothermal fluids using double-spike hydride generation MC-ICP-MS. *Geochim. Cosmochim. Acta* 70:3986–95. doi:10.1016/j.gca.2006.06.007
- Taylor, S. R., and S. M. McLennan. 1985. *The continental crust: Its composition and evolution*. Palo Alto, CA: Blackwell Scientific Pub.

- Wasson, J. T., and J. Kimberlin. 1966. Determination by neutron activation of gallium and germanium in iron meteorites. *Radiochim. Acta* 5:2193–99. doi:[10.1524/ract.1966.5.3.170](https://doi.org/10.1524/ract.1966.5.3.170)
- Weiss, D. J., M. Rehkdmper, R. Schoenberg, M. McLaughlin, J. Kirby, P. G. C. Campbell, T. Arnold, J. Chapman, K. Peel, and S. Gioia. 2008. Application of nontraditional stable-isotope systems to the study of sources and fate of metals in the environment. *Environ. Sci. Technol.* 42:655–64. doi:[10.1021/es0870855](https://doi.org/10.1021/es0870855)
- Xue, S., Y. L. Yang, G. S. Hall, and G. F. Herzog. 1997. Germanium isotopic compositions in Canyon Diablo spheroids. *Geochim. Cosmochim. Acta* 61:651–55. doi:[10.1016/S0016-7037\(96\)00363-8](https://doi.org/10.1016/S0016-7037(96)00363-8)
- Yang, L., and J. Meija. 2010. Resolving the germanium atomic weight disparity using multicollector ICPMS. *Anal. Chem.* 82:4188–93. doi:[10.1021/ac100439j](https://doi.org/10.1021/ac100439j)
- Yang, L., Z. Mester, L. Zhou, S. Gao, R. E. Sturgeon, and J. Meija. 2011. Observations of large mass-independent fractionation occurring in MC-ICPMS: Implications for determination of accurate isotope amount ratios. *Anal. Chem.* 83:8999–9004. doi:[10.1021/ac201795v](https://doi.org/10.1021/ac201795v)
- Yokoyama, T., A. Makishima, and E. Nakamura. 1999. Evaluation of the coprecipitation of incompatible trace elements with fluoride during silicate rock dissolution by acid digestion. *Chem. Geol.* 157:175–87. doi:[10.1016/S0009-2541\(98\)00206-X](https://doi.org/10.1016/S0009-2541(98)00206-X)
- Zhu, C.-w., H.-j. Wen, H.-f. Fan, Y.-x. Zhang, J. Liu, T. Yang, and G.-h. Wang. 2014. Chemical pre-treatment methods for measurement of Ge isotopic ratio on sphalerite in lead-zinc deposits. *Rock Miner. Anal.* 33:305–11. (in Chinese with English abstract)
- Zhu, J.-M., T. M. Johnson, S. K. Clark, and X.-K. Zhu. 2008. High precision measurement of selenium isotopic composition by hydride generation multiple collector inductively coupled plasma mass spectrometry with a  $^{74}\text{Se}$ - $^{77}\text{Se}$  double spike. *Chin. J. Anal. Chem.* 36:1385–90. doi:[10.1016/S1872-2040\(08\)60075-4](https://doi.org/10.1016/S1872-2040(08)60075-4)